American Journal of Reproductive Immunology

WILEY

AJRI
American Journal of Reproductive Immunology

ORIGINAL ARTICLE

Decreased IL-33 Expression in the Cervix in LPS-Induced Preterm Birth and the Potential Role of Mast Cells: A Murine Model

Sema Avci[1] | Ciler Celik-Ozenci[2,3] | Nilay Kuscu[4] | Nayce Ilayda Bektas[4]

[1]Department of Histology and Embryology, Alanya Alaaddin Keykubat University, School of Medicine, Antalya, Turkey | [2]Department of Histology and Embryology, Koc University, School of Medicine, Istanbul, Turkey | [3]Koc University Research Center for Translational Medicine (KUTTAM), Istanbul, Turkey | [4]Department of Histology and Embryology, Akdeniz University, School of Medicine, Antalya, Turkey

Correspondence: Sema Avci (sema.avci@alanya.edu.tr)

Received: 7 January 2025 | **Revised:** 2 April 2025 | **Accepted:** 21 April 2025

Funding: This research was supported by the Scientific and Technological Research Council of Turkey (TUBITAK, Project number 121S341, S.A.).

Keywords: cetirizine | IL-33 | inflammation | mast cell | preterm birth

ABSTRACT

Problem: In order to gain a deeper understanding of the mechanisms underlying LPS-mediated preterm birth, it is crucial to investigate the relationship between preterm birth and mast cells (MCs). Moreover, the role of antihistamines in inflammatory processes during pregnancy remains incompletely understood.

Method of Study: CD-1 female mice were administered intrauterine lipopolysaccharide (LPS) via midline laparotomy to establish an inflammation-induced preterm birth model. The experimental groups ($n = 6$ per group) were formed as Nonpregnant and pregnant control, Sham, PBS, LPS, Cetirizine (CET) control, and two CET treatment groups (CET 10 mg/kg-low dose, and CET 20 mg/kg-high dose with LPS administration). Tissue samples were analyzed using immunohistochemistry and Western blot techniques.

Results: Our findings suggest that MCs play a significant role in preterm birth, with LPS administration inducing MC dysfunction in the reproductive tract during pregnancy. Additionally, high doses of CET may support inflammatory responses. A particularly notable result was the reduction in interleukin-33 (IL-33) expression in the cervix during LPS-induced preterm birth. This suggests that IL-33 may serve as a potential biomarker for preterm birth in the cervix.

Conclusions: The effects of CET during LPS-mediated preterm birth appear to be dose-dependent, warranting further exploration of their role in this context.

1 | Introduction

Preterm birth is responsible for 75% of perinatal mortality and over 50% of long-term morbidity in neonates [1]. According to the World Health Organization, the incidence of preterm birth ranges from 4% to 16% [2]. Preterm labor is defined as the onset of labor before 37 weeks of gestation [3].

One of the most common mechanisms underlying preterm labor, particularly in cases associated with infection, is the increased

Abbreviations: CET, cetirizine; FcεRI, Fc epsilon receptor I; FcεRIα, high-affinity activating IgE receptor α-subunit; FcεRIβ, high-affinity activating IgE receptor β-subunit; HRH-1, histamine receptor H-1; LPS, lipopolysaccharide; McC, mast cell chymase; MCs, mast cells; McT, mast cell tryptase; Th2, T helper 2.

colonization of vaginal pathogens within the gestational cavity [4]. Furthermore, vaginal pathogens have been shown to reach the amniotic membrane, initiating an inflammatory response [5]. The cellular immune response plays a crucial role in combating these pathogens. Our previous study suggested that LPS induction may lead to changes in the activity of MCs [6].

Well-conserved markers are selectively expressed at various stages of MC lineage development. One such marker, the high-affinity IgE receptor (FcεRI), is crucial for studying this lineage [7]. FcεRI is a tetrameric receptor comprising an alpha (FcεRIα) subunit, which binds IgE, a beta (FcεRIβ) subunit, and two gamma (FcεRIγ) subunits. FcεRIα plays a pivotal role in allergic diseases by mediating the interaction between IgE and immune cells, such as MCs and basophils [8]. IgE antibodies are produced by mature B cells in response to signals from T helper 2 (Th2) cells [9].

A Th2-dominant cytokine profile is essential for supporting a successful pregnancy [10]. FcεRIγ, through its immunoreceptor tyrosine-based activation motifs (ITAMs), is vital for MC degranulation, cytokine production, prostaglandin synthesis, and the initiation of passive systemic anaphylaxis [11]. It has been proposed that type I hypersensitivity reactions, including histamine release, may contribute to the onset of preterm birth [12, 13].

Antihistamines have been used for more than three decades to treat allergic diseases, but their use is limited by sedation and anticholinergic side effects. Common side effects of first-generation antihistamines include sedation and anticholinergic effects. When the categorization of first-generation antihistamines by the FDA according to pregnancy complications is examined, it is seen that they generally fall into Category B/C [14, 15]. Second-generation antihistamines, such as CET, are characterized by their highly selective therapeutic index, long duration of action, and non-sedating properties. CET, a commonly used second-generation antihistamine, has been studied for its potential teratogenic effects and is classified as pregnancy Category B [16]. CET is a potent and specific H1 receptor antagonist and also has anti-inflammatory activities unrelated to histamine antagonism [17]. Second-generation H1 receptor antagonists are important first-line drugs for the relief of symptoms in patients with allergic rhinitis or chronic urticaria and have the potential to eventually replace sedating first-generation H1 receptor antagonists [18]. Additionally, studies have established a relationship between CET and teratogenicity and major malformations [19, 20]. CET was chosen as the preferred option for use during pregnancy due to the reasons outlined above regarding its fetal and maternal effects, as it appears to present a stronger possibility for use in pregnancy. It is also evident that more evidence and studies are needed regarding the use of antihistamines during pregnancy.

It has also been reported that CET may attenuate inflammatory cell migration in cutaneous reactions [21]. Studies have shown that no adverse effects were observed in infants breastfed by mothers who took 10 mg of CET orally [22]. Furthermore, CET has been suggested to possess anti-inflammatory properties, although the exact mechanism underlying this effect remains unclear. In an animal study involving rats treated with various analgesics, a dose of 5 mg/kg CET did not yield a significant effect, while doses of 10 and 20 mg/kg produced an experimental response [23]. Based on these findings, CET was chosen for our study and administered at the doses that elicited a measurable response in previous experiments.

Mast cell tryptase (McT), mast cell chymase (McC), cathepsin G, and carboxypeptidase are proteases stored in prepackaged granules within MCs, and these proteases facilitate the activation of metalloproteases in the extracellular matrix [24]. Alterations in the activities of tryptase and chymase are believed to play a significant role in pregnancy [25]. It has been reported that MCs are abundantly present in the uterus during pregnancy, and their composition is heterogeneous, with subsets expressing tryptase alone or both tryptase and chymase [26].

Cytokine alterations during pregnancy have been considered to be effective in the onset of preterm birth [27]. IL-33 is to play a key role in activating Th2 cells and MCs [28]. The receptor for IL-33, ST2, is expressed by leukocytes during inflammatory processes and has been shown to enhance cellular responsiveness to IL-33 [29]. ST2 is a member of the IL-1 superfamily, with IL-33 serving as its ligand [30]. Although the precise role of IL-33 in pregnancy remains incompletely understood, both IL-33 and its receptor, ST2, have been associated with adverse pregnancy outcomes, including recurrent pregnancy loss, preeclampsia, and preterm birth [31].

Although the literature on the status of surface markers and related factors of MCs LPS-mediated during preterm birth is limited, studies have indicated an increase in MCs in the cervix. However, their exact role in preterm or term birth remains inconclusive [25]. Further investigation into the complex interactions of MCs may provide new clinical approaches for managing a variety of pathological conditions [32]. Despite the existence of several studies on MCs, there is a notable lack of research that links MC mechanisms to preterm labor, especially in models where inflammation is induced within the uterine, cervical, and placental triangle. We hypothesize that dysfunction of MCs in the cervix, uterus, and placenta plays a critical role in the onset of LPS-mediated preterm birth.

2 | Material and Methods

2.1 | Experimental Design

Eight-twelve week-old female CD-1 mice in estrus, as determined by vaginal smear and appearance of the vaginal mucosa, were placed individually into separate cages with CD-1 male mice for mating. Mating was confirmed the following day by the presence of mating plugs, and plaque-positive females were considered to be pregnant, with a gestational age of 0.5 days.

The female mice were then assigned to one of the following experimental groups ($n = 6$ per group): Nonpregnant control **(NPC)**: Mice not exposed to pregnancy-related treatments. Pregnant control **(PC)**: Mice confirmed pregnant but not subjected to any additional treatments. **Sham**: Mice subjected to a sham treatment used to control for procedural effects. **PBS**: Mice treated with phosphate-buffered saline (PBS) as a vehicle control. **LPS**: Mice

treated with LPS, a known immune/inflammatory stimulant. CET control **(CET C)**: Mice treated with the compound CET (10 mg/kg) serve as a control group for CET treatment. LPS was not administered to the CET C group. **CET 10**: Mice treated with a low dose of CET (10 mg/kg) and LPS (25 μg). **CET 20**: Mice treated with a higher dose of CET (20 mg/kg) and LPS (25 μg). Each group was carefully monitored for subsequent experimental procedures based on their respective treatments, and the procedures are summarized in Drawing S1. Details regarding treatment are explained in the *treatment procedures* section.

2.2 | Treatment Procedures

LPS treatment (LPS; Sigma, Catalog #L2630, Escherichia coli O111) was administered as a single dose of 25 μg in 100 μL PBS via intrauterine (IU) injection. This treatment was used for the LPS group to induce an immune response. CET (Second-generation Histamine Receptor H-1 Antagonist) was administered in two doses of 10 mg/kg (dissolved in 100 μL PBS) by intraperitoneal (IP) injection at 10:00 a.m. on Days 13.5 and 14.5 of pregnancy in the CET C group and this group does not contain LPS. This dosing schedule was selected based on the pharmacokinetics of CET, considering the plasma peak level (1 h) [14] and its half-life (8 h) [33] as reported in previous studies. In the experimental groups receiving combined treatment (CET 10 and CET 20), CET was administered as described above (day of pregnancy13.5, 10:00 a.m. and 14.5, 10:00 a.m.), followed by the LPS injection at 14:00 on Day 14.5 of pregnancy. *Briefly:* CET 10 group received 10 mg/kg CET + 25 μg LPS (25 μg LPS in 100 μL PBS). CET 20 group received 20 mg/kg CET + 25 μg LPS (25 μg LPS in 100 μL PBS). In the Sham group, the peritoneum was surgically opened and closed without any additional treatment to control for surgical effects. In the PBS group, 100 μL of PBS was injected IU between two sacs to control the solvent and injection-related effects.

2.3 | Post-Treatment Care

After treatment, the animals were housed individually in standard cages. A 12-h light/dark cycle was maintained, with lights on from 07:00 to 19:00 and lights off from 19:00 to 07:00. Food and water were provided ad libitum, and the animals were monitored throughout the study for any adverse effects or behavioral changes following treatment

2.4 | Surgical Procedures

At 14.5 days of gestation, female mice were anesthetized using Avertin (2.5% tribromoethanol [T48402, Sigma] and 2.5% tert-amyl alcohol [240486, Sigma]) at a dose of 0.017 mL/kg body weight. A midline laparotomy was performed under sterile conditions. A 27-gauge needle was carefully inserted between the first and second sacs of the right uterine horn, closest to the cervix. A volume of 100 μL of either LPS or PBS, depending on the experimental group, was injected into the uterine sac. Following the injection, the peritoneum and surrounding tissue were sutured using a 4-0 Vicryl suture (Ethicon) to ensure proper healing.

2.5 | Exclusion Criteria

Subjects were excluded from the study based on the following criteria:

Body weight: If the average weight of the mice within a group deviated by more than 25% from the mean body weight, the subject was excluded. Number of pups: Mice with fewer than three fetuses in the uterus were excluded from the study. Adverse events: Mice that experienced significant delays in anesthesia induction, overuse of anesthetic, or insufficient LPS stimulation (none of the pups being premature) were also excluded. During the course of the experiment, two mice carrying fewer than three fetuses and one mouse that experienced severe stress following the procedure were euthanized and removed from the study. The removed mice have been replaced with new ones.

2.6 | Euthanasia and Tissue Collection Procedures

At 15.5 days post-coitus (dpc), euthanasia was performed via cervical dislocation. Following euthanasia, the cervix, uterus, and placenta tissues were excised for further analysis.

2.7 | Immunohistochemistry

After the tissue was harvested, the cervix, uterus, and placenta were fixed in 10% formalin fixative (Merck, Catalog #818708) for 24 h at room temperature. Following fixation, tissues were washed thoroughly with tap water and subsequently processed through a graded series of ethanol solutions (70%, 80%, and 90% ethanol; Sigma–Aldrich, Catalog #459844). Tissues were then incubated in 100% ethanol for 3 h, followed by clearing in xylene (Sigma–Aldrich, Catalog #534056) for approximately 5 min.

The tissues, which passed through paraffin and removed xylene, were embedded in clean paraffin. Once embedded, the tissues were sectioned to a thickness of 5 micrometers using a microtome. The sections were incubated overnight at 60°C to ensure proper adhesion to the slides. Following incubation, the slides were passed through xylene and a decreasing ethanol gradient (100%, 95%, 70%, 50%, and 30%) before being washed in 1X PBS (Sigma–Aldrich, Catalog #P4417-100TAB).

Before staining, the sections were treated with a citric acid buffer (Merck, Catalog #100244) for antigen retrieval. Sections were incubated with 3% hydrogen peroxide (H2O2; Sigma, Catalog #18312) for 10 min to block endogenous peroxidase activity. Afterward, Ultra V Block (Thermo Scientific, Catalog #TA-125-UB) was applied to reduce nonspecific binding.

2.8 | Antibodies

The following primary antibodies were used at a dilution of 1:100. Anti-Mast Cell Tryptase (Invitrogen, Catalog #ARC2328), Anti-Mast Cell Chymase (Invitrogen, Catalog #PA5-106362), Anti-FcεRIα (Abcam, Catalog #ab229889), Anti-FcεRIγ (Novus, Catalog #NBP3-04822), Anti-Histamine Receptor H1 (HRH1) (Invitrogen, Catalog #PA5-77463), Anti-ST2 (Abcam, Catalog

#ab25877), Anti-IL-33 (Abcam, Catalog #ab187060). Goat Anti-Rabbit (Vector, Catalog #BA-1000) at a dilution of 1:400 was used as a secondary antibody.

2.9 | Detection and Counterstaining

Diaminobenzidine (DAB, Sigma, Catalog #D4168) was used as the chromogen for antibody detection. Counterstaining was performed using Mayer's Hemalum Solution (Merck, Catalog #109249).

2.10 | Imaging

The immunostained sections were examined under a Zeiss Axioplan microscope (Germany), and images were captured with a Nikon MQD 42070 (4K) camera system (Japan). Images were evaluated at 5×, 20×, and 40× magnifications in the panels.

2.11 | Hematoxylin-Eosin Staining

Tissue sections were incubated at 60°C for the day and were deparaffinized by passing through xylene twice for 10 min each. The tissues were rehydrated by passing through a graded series of alcohols: 100%, 90%, 80%, and 70% ethanol, followed by a 5-min wash in distilled water.

Next, the sections were stained with Hematoxylin (Merck, Catalog #M105174.0500) for 1 min. After staining, the sections were washed in tap water for 5 min, allowing for the desired purple coloration to develop. The sections were then stained with Eosin (Merck, Catalog #1.15934) for 30 s.

Following the eosin staining, the sections were dehydrated by passing through 70%, 80%, and 90% ethanol for 1 s each, followed by incubation in 100% ethanol for 5 min. The tissues were then cleared in xylene twice for 10 min each. Finally, the slides were mounted with Entellan (Merck, Catalog #M107961.0100) to preserve the stained sections.

2.12 | Protein Extraction and Western Blot Analysis

Cervix, uterine, and placenta tissue lysates were prepared as described previously [34]. The primary antibodies were then applied to the membranes following the tissue preparation.

2.13 | Antibodies

Anti-Mast Cell Tryptase (Invitrogen, Catalog #ARC2328, 1:100, 30–35 kDa), Anti-Mast Cell Chymase (Invitrogen, Catalog #PA5-106362, 1:500, 28 kDa), Anti-FcεRIα (My Biosource, Catalog #MBS126480, 1:500, 68 kDa), Anti-FcεRIγ (Novus, Catalog #NBP3-04822, 1:200, 9 kDa), Anti-Histamine Receptor H1 (HRH1) (Proteintech, Catalog #13413-1-AP, 1:200, 56 kDa), Anti-ST2 (Invitrogen, Catalog #PA5-23316, 1:200, 28-38-66 kDa), Anti-IL-33 (Abcam, Catalog #ab187060, 1:400, 33 kDa). The Goat Anti-Rabbit secondary antibody (Abcam, Catalog #ab6721, 1:2000) was used to detect the primary antibodies. Beta-actin (Cell Signaling, Catalog #13E5, 1:2000, 45 kDa) was used as an internal control.

After the primary antibody incubation, membranes were washed with Tris-buffered saline with 0.1% Tween-20 (TBS-T) (Merck, Catalog #822184) and then incubated with the secondary antibody for 45 min at room temperature. Membranes were washed again with TBS-T, followed by incubation with Super Signal Chemiluminescence (CL)-HRP (Thermo Scientific, Catalog #A45918) for detection. Chemiluminescent signals were captured using the Azure Imaging Biosystem (Color C 600).

2.14 | Statistical Analysis

The subjects were assigned to tissue groups using a random number table in GraphPad Prism 9, allowing each subject's different tissues to be analyzed and represented by IHC or WB. Table S1, immunohistochemical staining intensity was evaluated blindly, and tissue-specific compartments were considered for each experimental group. The cervix, the transitional region, and the endocervical and ectocervical sections were examined. The placenta, the chorion, the labyrinth, the junctional zone, and the decidual areas were analyzed. The epithelium, stroma, and muscle and vascular structures present in these regions in the uterus, cervix, and placenta tissues were scored. For each marker in all experimental groups, three different areas from three randomly selected images of six subjects were analyzed. The intensity values were categorized, and power was graphed based on H-Score analysis, which showed −/+ (negative), + (mild), ++ (moderate), and +++ (severe) staining. Graphs were created by dividing the total value, obtained by assigning a numerical value between 0 and 3 according to the rating, by the number of measured compartments.

For Western blot analysis, protein and beta-actin band intensities were quantified using ImageJ software, and the protein/beta-actin ratios were statistically evaluated using GraphPad Prism v9 software. The homogeneity of the data was assessed using the Brown–Forsythe test. Differences between groups were analyzed using one-way ANOVA, followed by Holm-Sidak's multiple comparisons test for parametric data. A p value of <0.05 was considered statistically significant. Groups showing significant differences were marked with different letters in the relevant columns.

2.15 | Drawings

Illustrations were created using BioRender Scientific Image and Illustration Software.

3 | Results

The results of the procedures applied to the subjects and the observations made during the autopsies are summarized in supplementary (Figure 1A/a–o). Complete uterine emptying, ranging from 85% to 100%, was observed within 24 h only in the LPS-treated group (Figure 1A/p). All subjects were observed until 14:00, at which point euthanasia was performed. The birth process began around 06:00 the day after LPS administration. During

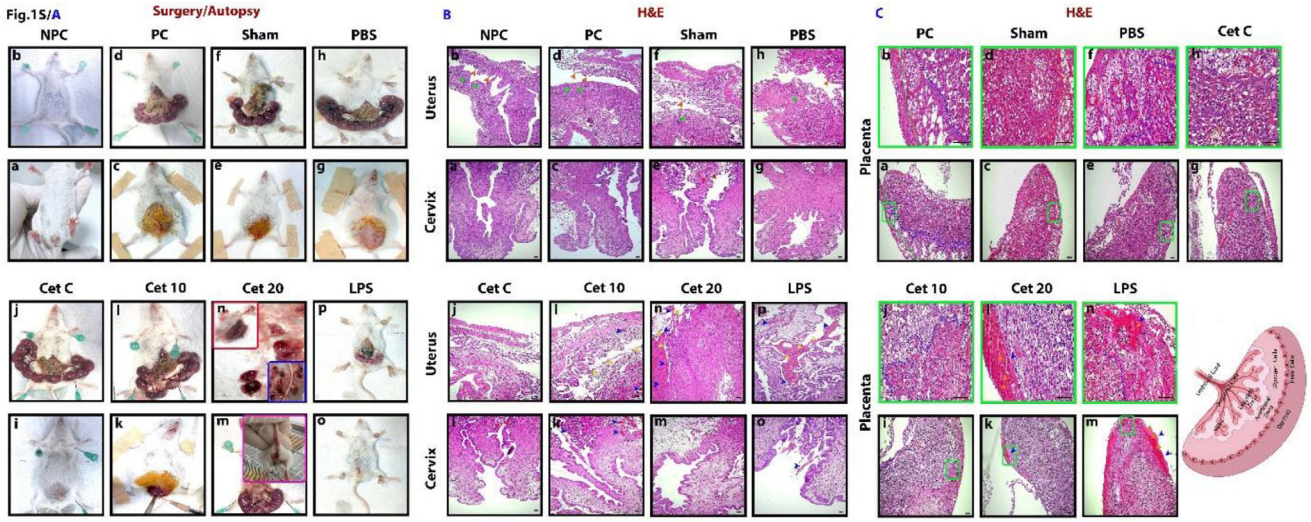

FIGURE 1 | (A) NPC (a,b): Nonpregnant control, PC (c,d): Pregnant control, Sham (e,f): Surgical control, PBS (g,h): Phosphate buffer solution, solvent control, Cet C (i,j): Cetirizine control, CET 10 (k,l): Cetirizine 10 mg/kg, CET 20 (m,n): Cetirizine 10 mg/kg, and LPS (o,p): Lipopolysaccharide, 25 μg/100 μL. Red frame: CET 20 fetal placenta, Blue Frame: Deteriorated and dead fetal structure, Pink Frame: Subject with the initiation of bleeding but showing an unsuccessful birth profile. (B) Evaluation of hematoxylin & eosin staining in cervix-uterus; the tissue appearance in the uterus where CET 20 and LPS are applied is similar. NPC (a,b): Nonpregnant control, PC (c,d): Pregnant control, sham (e,f): Surgical control, PBS (g,h): Phosphate buffer solution, solvent control, Cet C (i,j): Cetirizine control, CET 10 (k,l): Cetirizine 10 mg/kg, CET 20 (m,n): Cetirizine 20 mg/kg, and LPS (o,p): Lipopolysaccharide, 25 μg/100 μL. Orange arrowheads: uterine folds, green arrowheads: uterine cervix, blue arrowheads: blood vessels and bleeding areas, yellow arrowheads: infiltration areas and lymphocytes, and red arrowheads: transition zone from stratified squamous epithelium to prismatic epithelium. Scale bar: 50 μm. (C) Evaluation of hematoxylin & eosin staining in placenta; bleeding foci were observed in the decidual zone in the groups treated with LPS and CET 20 applied to the placenta. PC (a,b): Pregnant control, sham (c,d): Surgical control, PBS (e,f): Phosphate buffer solution, solvent control, Cet C (g,h): Cetirizine control, CET 10 (i,j): Cetirizine 10 mg/kg, CET 20 (k,l): Cetirizine 20 mg/kg, and LPS (m,n): Lipopolysaccharide, 25 μg/100 μL. Green dashed line: Boundary between decidual zone (DZ) and connecting zone (BZ), blue dashed line: Boundary between DZ and labyrinth zone (LZ), pink dashed line: Border between LZ and chorionic zone (CZ), and red dashed line: Glycogen islets. The image of the enlarged area was enclosed in the same color frame. The image of the magnified area was framed in the same color, Scale bar: 50 μm.

the observation period, each pup was immediately separated from the amniotic sac after birth, and the remaining placentas were harvested following euthanasia. Birth was observed in one subject in the CET 10 group, while preterm birth occurred in four subjects (Figure 1A/m-pink frame) in the CET 20 group. The difference in birth rates between the PC and LPS groups (Chi-square, p: 0.0003) and between the CET 10 and CET 20 groups (Chi-square, p: 0.0395) was significant. In the CET 10 group, the placental and fetal characteristics closely resembled those of the pregnant control group, whereas in the CET 20 group, the fetuses died earlier, similar to those in the LPS group (Figure 1A/n-blue frame). The placentas in the CET 20 group appeared larger, hemorrhagic, and exhibited color differences, particularly in areas facing the uterus (Figure 1A/n-red frame).

3.1 | Evaluation of Hematoxylin & Eosin Staining in Cervix-Uterus and Placenta

3.1.1 | The Tissue Appearance in the Uterus and Cervix Where CET 20 and LPS Are Applied Is Similar

The groups were examined for changes in the uterine folds (Figure 1B/b–h; orange arrowheads) and the cervix-uteri area (Figure 1B/b,f,h; green arrowheads). Bleeding foci (blue arrowheads) and lymphocyte infiltration (yellow arrowheads) were observed in the CET 10 (Figure 1B/k,l; blue and yellow arrowheads), CET 20 (Figure 1B/m,n; blue and yellow arrowheads) and only applied LPS groups (Figure 1B/o,p; blue and yellow arrowheads). Pregnant and CET C control groups were morphologically similar (Figure 1B/d–i). A clear change in epithelial morphology from stratified squamous to columnar epithelium was seen in the cervix-uterus transition zone (Figure 1B/e–i; red arrowheads).

3.1.2 | Bleeding Foci Were Observed in the Decidual Zone in the Groups Treated With LPS and Cet 20 Applied to the Placenta

The staining results show (Figure 1C/a–m) bleeding in the placental Decidual Zone (DZ) (Figure 1C/k–m; blue arrowheads), particularly in the CET 20 (Figure 1C/k,l) and LPS-treated groups (Figure 1C/m,n). The DZ- Junctional Zone (JZ) boundary (Figure 1C/b–n; green dashed line) and the DZ-Labyrinth Zone (LZ) boundary (Figure 1C/b–n; blue dashed line) are separated by the color line. The DZ-JZ boundary (Figure 1C/b–n; green dashed line) and the DZ-LZ boundary (Figure 1C/b–n; blue dashed line) are separated by a line. This suggests structural disruption or weakening between these placental zones in the treated groups. Glycogen islets (Figure 1C/b–n) are marked by red dashed lines in the sections. Their prominence or changes in appearance may indicate alterations in glycogen storage or metabolism in response to CET 20 and LPS treatments.

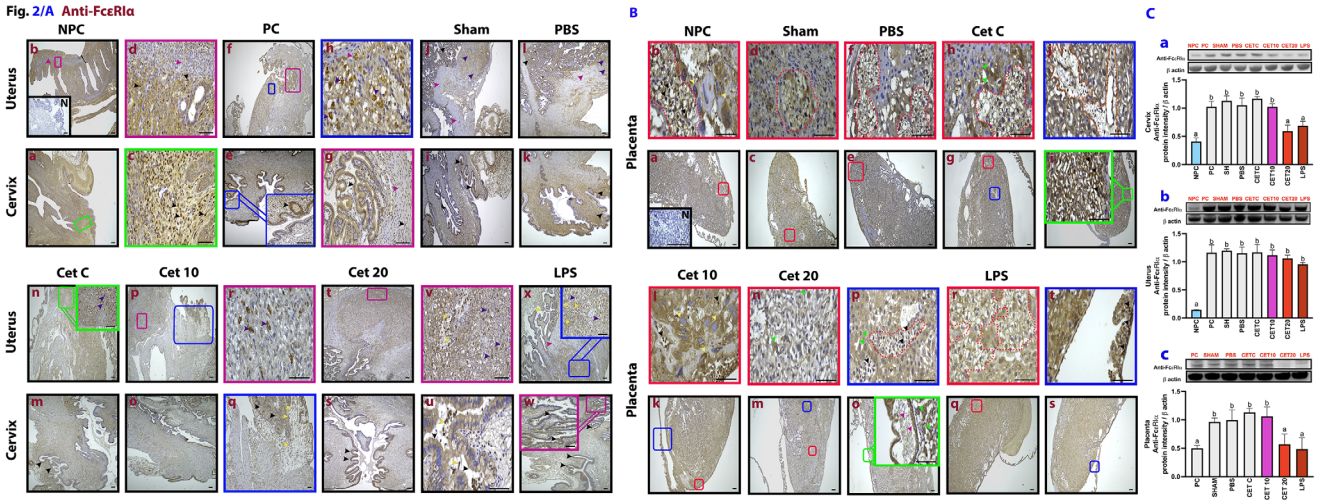

FIGURE 2 | (A) FcεRIα expression decreased in the cervix in CET 20 and LPS groups but remained unchanged in the uterus. NPC (a,d): Nonpregnant control, PC (e,h): Pregnant control, sham (i,j): Surgical control, PBS (k,l): Phosphate buffer solution, solvent control, Cet C (m,n): Cetirizine control, CET 10 (p–r): Cetirizine 10 mg/kg, CET 20 (t,v): Cetirizine 20 mg/kg, and LPS (w,x): Lipopolysaccharide, 25 μg/100 μL. Purple arrowheads: mast cells, black arrowheads: positively stained cells and structures, pink arrowheads: negatively stained cells and structures, and yellow arrowheads: infiltration areas and lymphocytes. The image of the magnified area was framed in the same color, N: Negative control, Scale bar: 50 μm. (B) FcεRIα expression decreased in the placenta of the CET 20 and LPS groups compared to the CET 10 group. PC (a,b): Pregnant control, sham (c,d): Surgical control, PBS (e,f): Phosphate buffer solution, solvent control, Cet C (g–j): Cetirizine control, CET 10 (k,l): Cetirizine 10 mg/kg, CET 20 (m–p): Cetirizine 20 mg/kg, and LPS (q–t): Lipopolysaccharide, 25 μg/100 μL. Black arrowheads: positively stained cell, green arrowheads: trophoblasts, yellow arrowheads: trophoblastic giant cells, blue arrowheads: blood vessels, red dashed line: glycogen islets, and orange dashed line: villus structure. The image of the magnified area was framed in the same color, N: Negative control, Scale bar: 50 μm. (C) FcεRIα protein levels decreased in the cervix in groups treated with LPS and CET 20, but remained unchanged in the uterus. In the placenta, expression was reduced in the LPS-treated group. (a–c): The amount of protein measured by Western blot.

3.2 | Immunohistochemistry of FcεRIα Protein in Cervix-Uterus and Placenta Tissues

3.2.1 | FcεRIα Expression Decreased in the Cervix in CET 20 and LPS Groups but Remained Unchanged in the Uterus

FcεRIα was positively expressed in the cervix epithelium and stroma (Figure 2A/c–x; black arrows). The uterine epithelium showed positive staining, which was more intense in the CET 20 and LPS groups (Figure 2A/s,x; black arrows) (Table S1a). MCs in the cervix and cervix uteri showed intense degranulation in all groups except for CET 20 and LPS groups (Figure 2A/h,j,l,n,r; purple arrows). In these latter groups, MC was notably weakened (Figure 2A/t–x; purple arrows). Lymphocyte infiltration was observed in CET 10, CET 20, and LPS groups (Figure 2A/q–x; yellow arrows). Cervical muscles showed no FcεRIα expression across all groups (Figure 2A/b–x; pink arrows).

3.2.2 | FcεRIα Expression Decreased in the Placenta of the CET 20 and LPS Groups Compared to the CET 10 Group

Placental trophoblastic giant cells stained positively in all groups (Figure 2B/b,l; yellow arrowheads). Glycogen islets in the CET 20 and LPS groups showed less intense staining (Figure 2B/p,r; red dashed line), whereas staining was more intense in other groups (Figure 2B/b–h; red dashed line). Notably, blood vessels in the chorionic zone (CZ) exhibited intense expression (Figure 2B/o; green frame and t; blue frame). Furthermore, FcεRIα expression in the yolk sac was strongly positive in the LPS group (Figure 2B/t; black arrowheads) (Table S1a).

3.3 | Western Blot Results of FcεRIα Protein

3.3.1 | FcεRIα Protein Levels Decreased in the Cervix in Groups Treated With LPS and CET 20 but Remained Unchanged in the Uterus. In the Placenta, Expression Was Reduced in the LPS-Treated Group

Our study demonstrated a significant decrease in FcεRIα protein levels in the CET 20 and LPS-treated groups, particularly in the cervix and placenta ($p < 0.05$) (Figure 2C/a,c). Although a reduction in staining intensity was observed in the CET 20 and LPS-treated groups across the cervix, uterus, and placenta, and this decrease was statistically significant in terms of protein levels only in the cervix and placenta (Figure 2C/a–c), but not in the uterus ($p > 0.05$) (Figure 2C/b).

3.4 | Immunohistochemistry of FcεRIγ Protein in Cervix-Uterus and Placenta Tissues

3.4.1 | FcεRIγ Levels Increased in the LPS and CET 20-Treated Groups, Particularly in the Epithelial Regions of the Cervix and Uterus

In all groups, FcεRIγ was more intensely expressed in some stromal cells in the cervix and uterus (Figure 3A/a–d; black

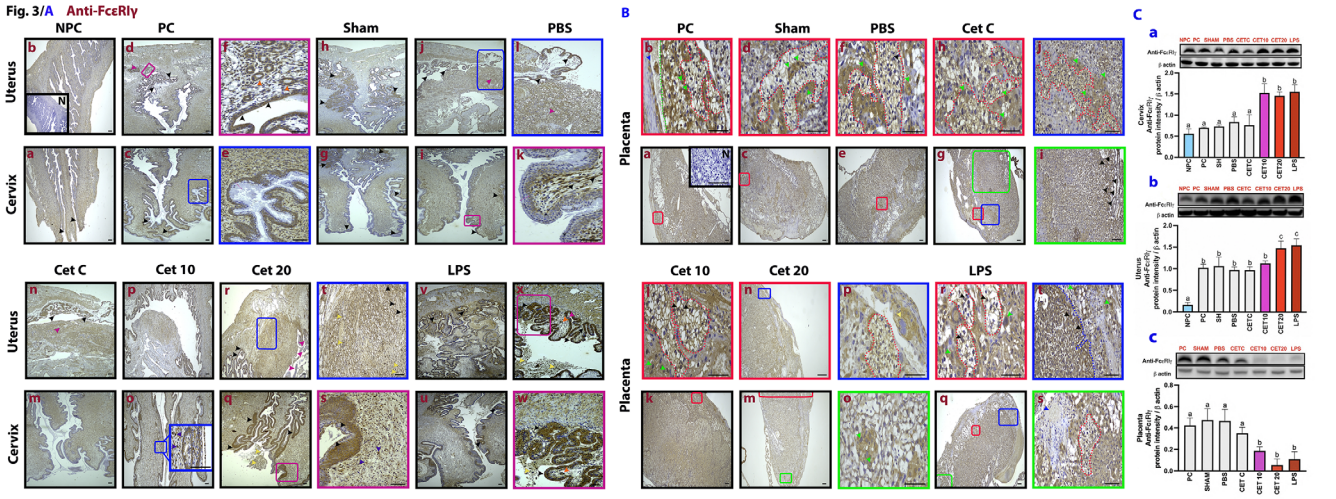

FIGURE 3 | (A) FcεRIγ levels increased in the LPS- and CET 20-treated groups, particularly in the epithelial regions of the cervix and uterus. NPC (a,b): Nonpregnant control, PC (c–f): Pregnancy control, sham (h–j): Surgical control, PBS (k,l): Phosphate buffer solution, solvent control, Cet C (m,n): Cetirizine control, CET 10 (o,p): Cetirizine 10 mg/kg, CET 20 (q–t): Cetirizine 20 mg/kg, and LPS (v,x): Lipopolysaccharide, 25 μg/100 μL. Purple arrowheads: mast cells, black arrowheads: positively stained cells and structures, pink arrowheads: negatively stained cells and structures, and yellow arrowheads: infiltration areas and lymphocytes. The image of the magnified area was framed in the same color, N: Negative control, Scale bar: 50 μm. (B) FcεRIγ expression was decreased in all zones of the placenta in the groups treated with LPS and CET 20. PC (a,b): Pregnant control, sham (c,d): Surgical control, PBS (e,f): Phosphate buffer solution, solvent control, Cet C (g–j): Cetirizine Control, CET 10 (k,l): Cetirizine 10 mg/kg, CET 20 (m–p): Cetirizine 20 mg/kg, and LPS (q–t): Lipopolysaccharide, 25 μg/100 μL. Black arrowheads: positively stained cell, green arrowheads: spongiotrophoblast, blue arrowheads: blood vessels, yellow arrowheads: trophoblastic giant cells, red dashed line: glycogen islets, blue dashed line: BZ and LZ boundary. The image of the magnified area was framed in the same color, N: Negative control, Scale bar: 50 μm. (C) FcεRIγ protein levels increased in the cervix and uterus in the groups treated with LPS and CET 20, while a decrease was observed in the placenta in these groups. (a–c): The amount of protein measured by Western blot.

arrows), in the basal compartment of the epithelium lining the cervix (Figure 3A/c,e,g,i,q,s,u,w; black arrows, e,k; pink dashed line), and in the uterine epithelium (Figure 3A/d,f,h,o,t,x,*; black arrows) (Table S1b). Additionally, FcεRIγ was positively stained in glandular structures (Figure 3A/x,w; orange arrows).

Some cells within the expression areas did not exhibit staining (Figure 3A/d–w; pink arrows). Areas of lymphocyte infiltration were notably intense in the CET 20 group (Figure 3A/q–t yellow arrowheads). MC expression in the uterine body increased in the CET 10, CET 20, and LPS groups compared to the control groups (Figure 3A/o,s; purple arrows).

3.4.2 | FcεRIγ Expression Was Decreased in All Zones of the Placenta in the Groups Treated With LPS and CET 20

FcεRIγ staining was weak in glycogen islets across all groups in the placenta (Figure 3B/b-l; red dashed lines and black arrowheads). Intense staining was observed in spongiotrophoblasts within the JZ in the control groups (Figure 3B/b–l; green arrowheads). However, this staining was reduced in the CET 20 and LPS-treated groups around giant trophoblastic cells (Figure 3B/p; yellow arrowheads) and spongiotrophlasts (Figure 3B/o–t; green arrowheads). Additionally, positive staining in blood vessels decreased in the CET 20 and LPS-treated groups (Figure 3B/b,s; blue arrowheads). FcεRIγ expression in the LZ remained similar in the LPS group compared to other groups (Figure 3B/t; blue dashed line) (Table S1b).

3.5 | Western Blot Results of FcεRIγ Protein

3.5.1 | FcεRIγ Protein Levels Increased in the Cervix and Uterus in the Groups Treated With LPS and CET 20, While a Decrease Was Observed in the Placenta in these Groups

The significant increase in FcεRIγ protein levels in the cervix ($p < 0.05$) (Figure 3C/a) in the CET 20 and LPS-treated groups is thought to be associated with the regulation of cytokine and prostaglandin production mediated by the Th2 response. This increase was also significant in the uterus in the CET 20 and LPS groups ($p < 0.05$) (Figure 3C/b). Conversely, the decrease in immunohistochemical expression observed in the placenta, particularly in the labyrinth zone in the CET 20 and LPS groups, was mirrored at the protein ($p < 0.05$) (Figure 3C/c) (Table S1b).

3.6 | Immunohistochemistry of HRH-1 Protein in Cervix, Uterus, and Placenta Tissues

3.6.1 | The Expression of HRH-1 Was Markedly Reduced in the CET 20 Group, Resembling the Pattern Observed in the LPS-Treated Group, Particularly in the Cervix and Uterus. In Contrast, the CET 10 Group Exhibited Intense HRH-1 Expression at the Basal Layer of the Cervical Epithelium and Within the Cervix Uteri

Muscle tissue did not demonstrate any staining in all experimental groups (Figure 4A/b–w; pink arrowheads). Conversely, positive staining was observed in the uterine

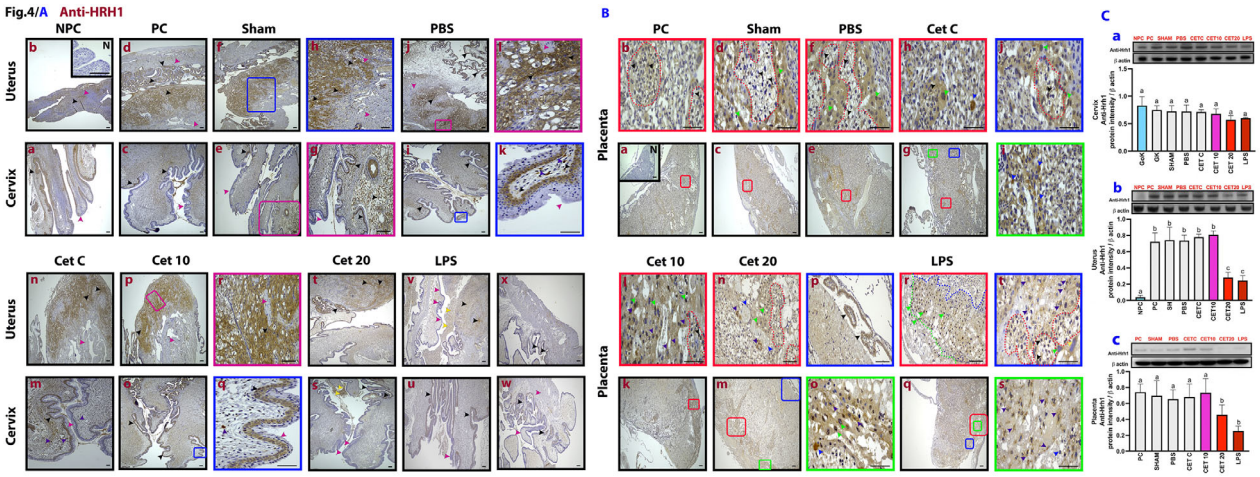

FIGURE 4 | (A) The expression of HRH-1 was markedly reduced in the CET 20 group, resembling the pattern observed in the LPS-treated group, particularly in the cervix and uterus. In contrast, the CET 10 group exhibited intense HRH-1 expression at the basal layer of the cervical epithelium and within the cervix uteri. NPC (a,b): Nonpregnant control, PC (c,d): Pregnant control, sham (e–h): Surgical control, PBS (i–l): Phosphate buffer solution, solvent control, Cet C (m,n): Cetirizine Control, CET 10 (o–r): Cetirizine 10 mg/kg, CET 20 (t,s): Cetirizine 20 mg/kg, and LPS (v–x): Lipopolysaccharide, 25 μg/100 μL. Purple arrowheads: mast cells, black arrowheads: cells and structures that stain positively, pink arrowheads: cells and structures that stain negatively, and yellow arrowheads: infiltration areas and lymphocytes. The image of the magnified area was framed in the same color, N: Negative control, Scale bar: 50 μm. (B) HRH-1 expression in the placenta was reduced in the LPS and CET 20 groups. PC (a,b): Pregnant control, sham (c,d): Surgical control, PBS (e,f): Phosphate buffer solution, solvent control, Cet C (g–j): Cetirizine control, CET 10 (k,l): Cetirizine 10 mg/kg, CET 20 (m–p): Cetirizine 20 mg/kg, and LPS (q–t): Lipopolysaccharide, 25 μg/100 μL. Black arrowheads: positively stained cell, green arrowheads: spongiotrophoblast, blue arrowheads: blood vessels, purple arrowheads: mast cells, red dashed line: glycogen islets. The image of the magnified area was framed in the same color, N: Negative control, Scale bar: 50 μm. (C) While the HRH-1 protein level in the cervix did not change between the groups, it decreased in the uterus in the groups treated with LPS and CET 20. The change in the placenta was similar to that observed in the uterus. (a–c): The amount of protein measured by Western blot.

epithelium (Figure 4A/b–x; black arrowheads) and cervical epithelium, predominantly localized in the basal areas (Figure 4A/a–x; black and pink arrowheads). No staining was detected on the epithelial surface (Figure 4A/m,q; pink arrowheads). Notably, both the CET 20 and LPS groups exhibited reduced uterine cervical staining (Figure 4A/t–v; black arrowheads) (Table S1c).

Positive staining was evident in regions of lymphocyte infiltration in the CET 20 and LPS groups (Figure 4A/s,v; yellow arrowheads). MCs in the cervical orifice displayed positive staining in the control groups (Figure 4A/k,m,q; purple arrowheads); however, these cells were weakly stained in the uterine cervix in the CET 20 and LPS groups. Both visible MC counts and staining intensity were diminished in the CET 20 and LPS groups (Figure 4A/s–u). Additionally, a reduction in epithelial staining intensity was observed in the LPS group compared to the control groups (Figure 4A/v,w; pink arrowheads) (Table S1c).

3.6.2 | HRH-1 Expression in the Placenta Was Reduced in the LPS and CET 20 Groups

The staining intensity in glycogen islets (Figure 4B/n–u; red dashed line and black arrowheads) was diminished in the CET 20 and LPS groups compared to the other groups (Figure 4B/b-1; red dashed line and black arrowheads). Similarly, the staining intensity in blood vessels was reduced in the CET 20 and LPS groups (Figure 4B/h,i; blue arrowheads) and (Figure 4B/n-t; blue arrowheads). Staining around the spongiotrophoblasts was generally intense, except in the CET 20 and LPS groups (Figure 4B/b-1; green arrowheads), where these structures exhibited reduced staining (Figure 4B/n–u; green arrowheads). However, granular structures of MCs surrounding the spongiotrophoblasts (Figure 4B/d–j; green arrowheads) stained positively. The granules showed stronger positive staining in the LPS, CET 10, and CET 20 groups, and spongiotrophoblast nuclei were similarly stained (Figure 4B/l–u; purple arrowheads). MCs located near the decidua in these groups displayed degranulation (Figure 4B/l–u; purple arrowheads). Additionally, staining in the yolk sac was positive, and intense expression was observed in the labyrinth and junctional zone of the placenta (Table S1c).

3.7 | Western Blot Results of HRH-1 Protein

3.7.1 | While the HRH-1 Protein Level in the Cervix Did Not Change Between the Groups, It Decreased in the Uterus in the Groups Treated With LPS and CET 20. The Change in the Placenta Was Similar to That Observed in the Uterus

The HRH-1 protein was expressed in the cervix and placenta during the pregnancy period. Its expression, which was weak in the uterus before pregnancy, increased during pregnancy (Figure 4C/a,c). However, in the CET 20 group, HRH-1 expression decreased significantly in all tissues, similar to the LPS group ($p < 0.05$) (Figure 4C/a–c). Notably, the reduction in protein levels in the uterus and placenta was significant ($p < 0.05$) (Figure 4C/a,c).

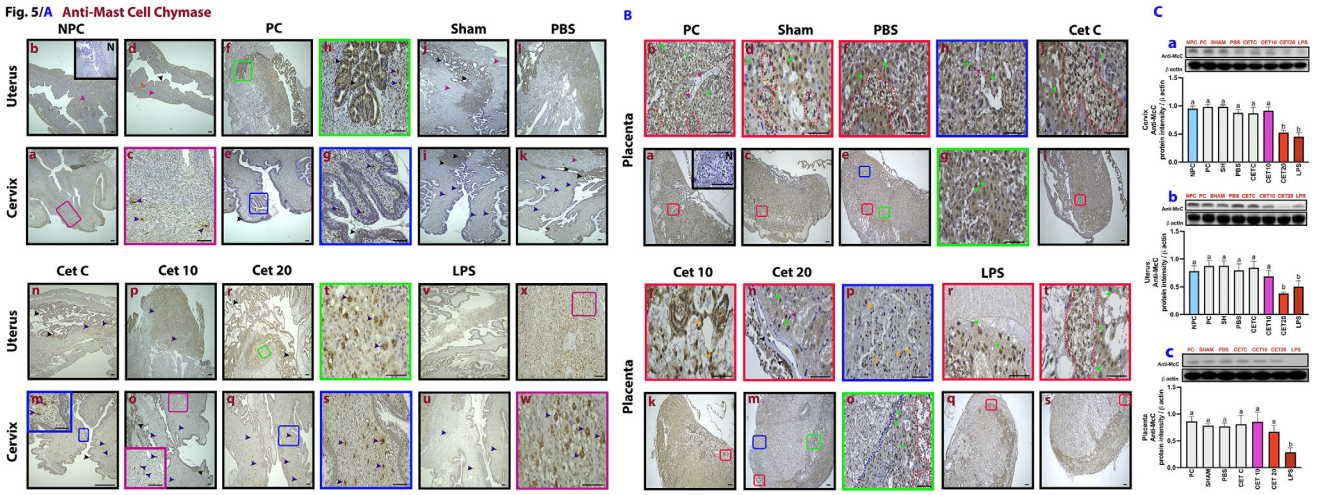

FIGURE 5 | (A) McC expression was decreased in the cervix and uterus in the LPS and CET 20 groups, with the reduction being particularly evident in the cervix. NPC (a–d): Nonpregnant control, PC(e–h): Pregnant control, sham (k,l): Surgical administration control, PBS (k,m): Phosphate buffer solution, solvent control, Cet C (m,n): Cetirizine control, CET 10 (o,p): Cetirizine 10 mg/kg, cetirizine 20 (r–t): Cetirizine 20 mg/kg, and LPS (v–x): Lipopolysaccharide, 25 μg/100 μL. Black arrowheads: positive staining cells and structures, purple arrowheads: mast cells, orange arrowhead: uterine gland structures, and pink arrowheads: cells and structures that stain negatively. The image of the magnified area is framed in the same color, N: Negative control, Scale bar: 50 μm. (B) McC expression was decreased in the placenta in the LPS and CET 20 groups, similar to its reduction in other tissues. This decrease was particularly evident in the LZ. PC (a,b): Pregnant control, sham (c,d): Surgical control, PBS (e,h): Phosphate buffer solution, solvent control, Cet C (i–j): Cetirizine Control, CET 10 (k,l): Cetirizine 10 mg/kg, CET 20 (m–p): Cetirizine 20 mg/kg, and LPS (q–t): Lipopolysaccharide, 25 μg/100 μL. Black arrowheads: positive stained cells and structures, green arrowheads: spongiotrophoblast, pink arrowheads: cells and structures that stain negatively, yellow arrowheads: trophoblastic giant cells, orange arrowheads: sinusoidal trophoblasts, and red dashed line: glycogen islets. The image of the enlarged area was enclosed in the same color frame. Blue dashed line: BZ and LZ border, N: Negative control, Scale bar: 50 μm. (C) McC protein levels were decreased in the cervix and uterus in the LPS and CET 20 groups. In the placenta, the decrease was observed only in the LPS group. In the CET 10 group, the protein levels in all tissues were similar to those in the control group. (a–c): The amount of protein measured by Western blot.

3.8 | Immunohistochemistry of McC Protein in Cervix-Uterus and Placenta Tissues

3.8.1 | McC Expression Was Decreased in the Cervix and Uterus in the LPS and CET 20 Groups, With the Reduction Being Particularly Evident in the Cervix

In the control groups, McC staining was intense in the cervical orifice and the uterine cervix (Figure 5A/c–w; purple arrowheads). However, the expression intensity of these cells was significantly decreased in the CET 20 and LPS groups (Figure 5A/q–w; purple arrowheads). In the control groups, staining was positive on the surface (Figure 5A/d–m; black arrowheads) and in the glandular epithelium (Figure 5A/d; orange arrowheads). In contrast, staining was notably reduced in the CET 20 group (Figure 5A/r–t; purple and black arrowheads) and the LPS group (Figure 5A/u–w; purple and black arrowheads) (Table S1d).

3.8.2 | McC Expression Was Decreased in the Placenta in the LPS and CET 20 Groups, Similar to Its Reduction in Other Tissues. This Decrease Was Particularly Evident in the LZ

In the placenta, McC expression was concentrated in the spongiotrophoblasts (Figure 5B/a–j; green arrowheads) and glycogen islets (Figure 5B/d–j; red dashed line) in the control groups. However, expression was reduced in the LZ in the CET 20 (Figure 5B/m,o; above and below the blue dashed line, green arrowheads) and LPS (Figure 5B/q,s; green arrowheads) groups. On the other hand, staining in spongiotrophoblasts increased in the JZ (Table S1d). No expression was observed in the blood vessels (Figure 5B/b,h; pink arrowheads). In the CET applied groups, expression was positive in the sinusoidal trophoblasts (Figure 5B/l–p; orange arrowheads). Staining in glycogen islets was reduced in the CET 20 (Figure 5B/o; red dashed line) and LPS (Figure 5B/t; red dashed line) groups compared to the control groups.

3.9 | Western Blot Results of McC Protein

3.9.1 | McC Protein Levels Were Decreased in the Cervix and Uterus in the LPS and CET 20 Groups. In the Placenta, the Decrease Was Observed Only in the LPS Group. In the CET 10 Group, the Protein Levels in all Tissues Were Similar to Those in the Control Group

The decrease observed at the tissue level in the epithelium and stroma of the cervix and uterus in the LPS and CET 20 groups was consistent with the decrease at the protein level ($p < 0.05$) (Figure 5C/a,b). In the placenta, the reduction in staining intensity observed in the CET 20 and LPS groups, particularly in the LZ and CZ, was significantly similar to the protein level decrease in the LPS group ($p < 0.05$) (Table S1d and Figure 5C/c).

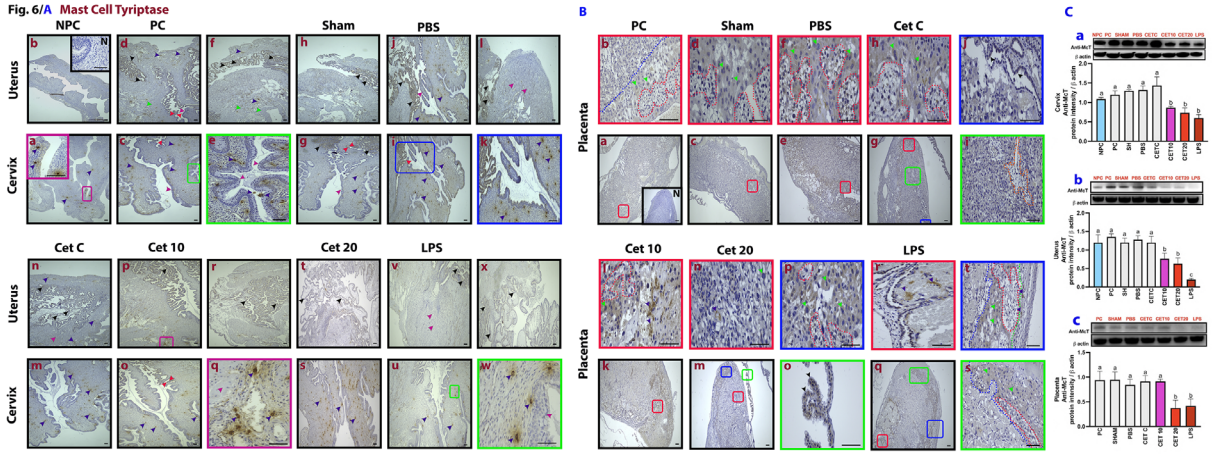

FIGURE 6 | (A) McT expression was decreased in LPS and CET 20 groups. NPC (a,b): Nonpregnant control, PC (d–f): Pregnant control, sham (g,h): Surgical control, PBS (i–l): Phosphate buffer solution, solvent control, Cet C (m,n): Cetirizine control, CET 10 (p–r): Cetirizine 10 mg/kg, CET 20 (s,t): Cetirizine 20 mg/kg, and LPS (u–x): Lipopolysaccharide, 25 μg/100 μL. Black arrowheads: positive staining cells and structures, purple arrowheads: mast cells, pink arrowheads: negative staining cells and structures, and red arrowheads: transition region from stratified squamous epithelium to columnar epithelium. The image of the magnified area was framed in the same color, N: Negative control, Scale bar: 50 μm. (B) McT expression in the placenta was decreased in the LPS and CET 20 groups, similar to the reductions observed in the cervix and uterus tissues. PC (a,b): Pregnant control, sham (c,d): Surgical control, PBS (e,f): Phosphate buffer solution, solvent control, Cet C (g–j): Cetirizine Control, CET 10 (k,l): Cetirizine 10 mg/kg, CET 20 (m–p): Cetirizine 20 mg/kg, and LPS (q–t): Lipopolysaccharide, 25 μg/100 μL. Black arrowheads: positive stained cells and structures, green arrowheads: spongiotrophoblast, purple arrowheads: mast cells, orange dashed line: villus, and red dashed line: glycogen islets. The image of the enlarged area was enclosed in the same color frame. Blue dashed line: BZ and LZ boundary. N: Negative control, Scale bar: 50 μm. (C) McT protein levels decreased in all groups treated with LPS in the cervix and uterus. The decrease in the placenta was limited to the LPS and CET 20 groups, while the CET 10 group showed protein levels similar to the controls. (a–c): The amount of protein measured by Western blot.

3.10 | Immunohistochemistry of McT Protein in Cervix-Uterus and Placenta Tissues

3.10.1 | McT Expression Was Decreased in the LPS and CET 20 Groups

Staining was weak in the cervical epithelium (Figure 6A/c–g; pink arrowheads), whereas staining was positive in the uterine epithelium (Figure 6A/d–n; black arrowheads). Expression increased after a certain point in the transition zone during pregnancy (Figure 6A/d–i; red arrowheads). All pregnant control groups showed weak expression in the cervix uteri (Figure 6A/l,n; pink arrowheads), while the CET 20 and LPS groups showed negative staining (Figure 6A/v,w; pink arrowheads). The staining pattern in pregnant controls (Figure 6A/c–n) and the CET 10 group (Figure 6A/p–r) was similar in the uterus. In contrast, uterine epithelial staining was weakened in the CET 20 (Figure 6A/t,s) and LPS groups (Figure 6A/v,x). MCs were intensely observed in the cervix in all groups except the LPS group (Figure 6A/a–w; purple arrowheads) (Table S1e).

3.10.2 | McT Expression in the Placenta Was Decreased in the LPS and CET 20 Groups, Similar to the Reductions Observed in the Cervix and Uterus Tissues

In the placenta, spongiotrophoblasts (Figure 6B/a–h; green arrowheads), glycogen islets (Figure 6B/a–h; red dashed line), chorion epithelium (Figure 6B/j; black arrowheads and, to a lesser extent, villi (Figure 6B/i; orange dashed line) showed positive staining. While staining in spongiotrophoblasts was similar in the LPS-treated groups (Figure 6B/s,t; green arrowheads), expression was decreased in the LZ (Figure 6B/s,t; blue dashed underline). In these groups, cells with positive expression were observed in the chorion (Figure 6B/r; purple arrowheads) and decidua vessels (Figure 6B/t; purple arrowheads). Staining was positive in the yolk sac, but the staining intensity was weak in glycogen islets in the LPS group (Figure 6B/s,t; red dashed line) (Table S1e).

3.11 | Western Blot Results of McT Protein

3.11.1 | McT Protein Levels Decreased in all Groups Treated With LPS in the Cervix and Uterus. The Decrease in the Placenta Was Limited to the LPS and CET 20 Groups, While the CET 10 Group Showed Protein Levels Similar to the Controls

McT levels were significantly decreased in the cervix and uterus in the LPS-treated groups ($p < 0.05$). In the placenta, protein levels in the CET 10 group were similar to those in the control group (Figure 6C/a–c).

3.12 | Immunohistochemistry of IL-33 Protein in Cervix-Uterus and Placenta Tissues

3.12.1 | IL-33 Expression Was Intensely Observed in the Epithelial Tissue, Particularly in the External os of the Cervix, With a Dramatic Reduction in the LPS Group

As a notable result of our study, IL-33 was strongly expressed in the cervical epithelium but weakly expressed in the uterus

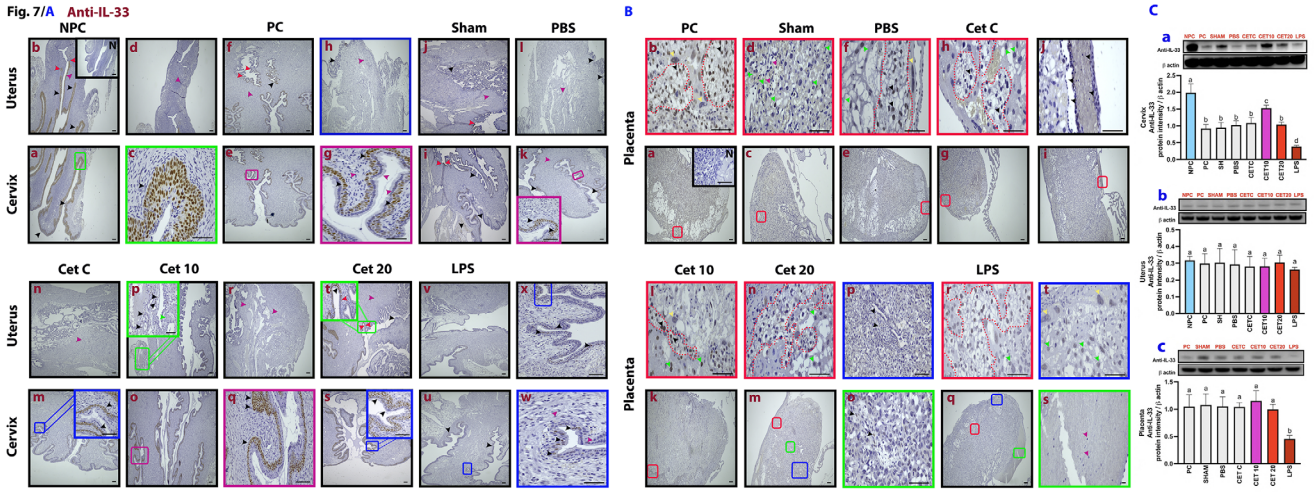

FIGURE 7 | (A) IL-33 expression was intensely observed in the epithelial tissue, particularly in the external os of the cervix, with a dramatic reduction in the LPS group. NPC (a,d): Nonpregnant control, PC (f–h): Pregnant control, sham (i,j): Surgical control, PBS (k,l): Phosphate buffer solution, solvent control, Cet C (m,n): Cetirizine control, CET 10 (p–r): Cetirizine 10 mg/kg, CET 20 (t,s): Cetirizine 20 mg/kg, LPS (v–x): Lipopolysaccharide, 25 μg/100 μL. Black arrowheads: positively stained cells and structures, pink arrowheads: negatively stained cells and systems, and red arrowheads: transition region from stratified squamous epithelium to prismatic epithelium. The image of the magnified area was framed in the same color, N: Negative control, Scale bar: 50 μm. (B) Placental IL-33 expression was decreased in the LPS and CET 20 groups. PC (a,b): Pregnant control, sham (c,d): Surgical control, PBS (e,f): Phosphate Buffer Solution, solvent control, Cet C (g–j): Cetirizine Control, CET 10 (k,l): Cetirizine 10 mg/kg, CET 20 (m–p): Cetirizine 20 mg/kg, and LPS (q–t): Lipopolysaccharide, 25 μg/100 μL. Black arrowheads: positively stained cells and structures, green arrowheads: spongiotrophoblast, yellow arrowheads: trophoblastic giant cells, pink arrowheads: negatively stained cells and structures, and red dashed line: glycogen islets. The image of the enlarged area was enclosed in the same color frame. N: Negative control, Scale bar: 50 μm. C: IL-33 protein levels were decreased in the cervix and placenta in the LPS group, while no significant change was observed in the uterus. (a–c): The amount of protein measured by Western blot.

(Figure 7A/a–n; black and pink arrowheads) (Table S1f). In all pregnant groups except LPS, IL-33 was intensely expressed below a specific point in the cervix (Figure 7A/a; black arrowheads) and in the transition zone (Figure 7A/b; red arrowheads). During pregnancy, uterine expression increased in the epithelial layer (Figure 7A/f–k; black arrowheads). No staining was observed in the stromal areas (Figure 7A/b–w; pink arrowheads). However, epithelial staining in the cervix and uterus was reduced in the CET 20 and LPS groups (Figure 7A/t,x; black arrowheads) (Table S1f).

3.12.2 | Placental IL-33 Expression Was Decreased in the LPS and CET 20 Groups

In the control groups, IL-33 staining was positive in LZ trophoblasts (Figure 7B/a,c,e,g), glycogen islets (Figure 7B/b–h; red dashed line), trophoblastic giant cells (Figure 7B/b–f; yellow arrowheads), and spongiotrophoblasts (Figure 7B/d–h; green arrowheads). The staining pattern in the CET 10 group was similar to the controls (Figure 7B/k,l; green and yellow arrowheads). However, in the CET 20 group, staining intensity decreased in glycogen islets (Figure 7B/n; red dashed line), spongiotrophoblasts (Figure 7B/n; green arrowheads), and the LZ (Figure 7B/o,p; black arrowheads). In the LPS group, staining intensity in all these structures was the lowest compared to other groups (Figure 7A/r–t; green and yellow arrowheads, red dashed line). Neutrophils exhibited negative staining (Figure 7B/s; pink arrowheads) (Table S1f).

3.13 | Western Blot Results of IL-33 Protein

3.13.1 | The Levels of IL-33 Protein Were Significantly Reduced in the Cervix and Placenta in the LPS Group, While no Significant Change Was Observed in the Uterus

The decrease in protein levels in the cervix and placenta in the LPS group was statistically significant ($p < 0.05$), whereas the difference in the uterus was not significant (Figure 7C/a–c). Furthermore, in the CET 10 group, the increase in IL-33 expression in the cervix at the protein level was also significant ($p < 0.05$) (Figure 7C/a).

3.14 | Immunohistochemistry of St2 Protein in Cervix-Uterus and Placenta Tissues

3.14.1 | In the LPS and CET 20 Applied Groups, St-2 Expression Was Unchanged in the Cervix and Increased in the Uterine Epithelium

St-2 staining intensity was weak in the cervical opening of the NPC group (Figure 8A/a; black arrowhead), as well as in the uterine and glandular epithelium (Figure 8A/c; orange arrowheads). Expression increased in the uterine epithelium and cervix uteri during pregnancy (Figure 8A/f–n; black arrowheads). Staining was particularly evident in MCs in the cervix uteri (Figure 8A/g–n; purple arrowhead). In the CET 20 and LPS groups, staining intensity in the epithelium was increased (Figure 8A/r–x; black

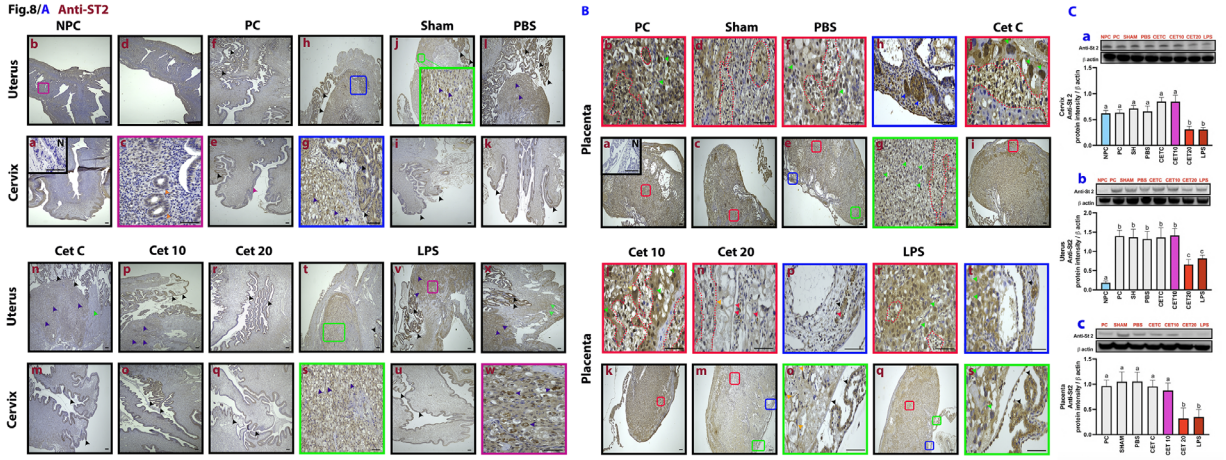

FIGURE 8 | (A) Expression of St-2 was intense in the cervix and uterine epithelium in the LPS- and CET 20-treated groups. NPC (a–d): Nonpregnant control, PC (f–h): Pregnant control, sham (i,j): Surgical application control, PBS (k,l): Phosphate buffer solution, solvent control, Cet C (m,n): Cetirizine control, CET 10 (o,p): Cetirizine 10 mg/kg, CET 20 (q–t): Cetirizine 20 mg/kg, and LPS (u–x): Lipopolysaccharide, 25 μg/100 μL. Purple arrowheads: mast cells, black arrowheads: positive stained cells and structures, orange arrowhead: uterine gland structures, and green arrowheads: uterine muscle structures. The image of the augmented area was framed in the same color, N: Negative control, Scale bar: 50 μm. (B) St2 expression was decreased in placental tissue in the LPS and CET 20 groups, with the decrease being particularly evident in the LZ. PC (a,b): Pregnant control, sham (c,d): Surgical control, PBS (e,h): Phosphate buffer solution, solvent control, Cet C (i–j): Cetirizine control, CET 10 (k,l): Cetirizine 10 mg/kg, CET 20 (m–p): Cetirizine 20 mg/kg, and LPS (q–t): Lipopolysaccharide, 25 μg/100 μL. Black arrowheads: positive stained cells and structures, green arrowheads: spongiotrophoblast, yellow arrowheads: trophoblastic giant cells, red arrowheads: hematopoietic blood cells, orange arrowheads: sinusoidal trophoblasts, blue arrowheads: blood vessels, and red dashed line: glycogen islands. The image of the magnified area was enclosed in the same color frame. N: Negative control, Scale bar: 50 μm. (C) St2 protein levels were decreased in the cervix, uterus, and placenta in the groups treated with LPS and CET 20. (a–c): The amount of protein measured by Western blot.

arrowheads) (Table S1g). Muscle staining, which was weak in the control groups and increased in the LPS-treated groups (Figure 8A/n–x; green arrowheads) (Table S1g).

3.14.2 | St2 expression Was Decreased in Placental Tissue in the LPS and CET 20 Groups, With the Decrease Being Particularly Evident in the LZ

In the control and CET 10 groups, St2 staining in the placenta was intense in spongiotrophoblasts (Figure 8B/a-1; green arrowheads), trophoblastic giant cells (Figure 8B/j,1; yellow arrowheads), glycogen islets (Figure 8B/a-1; red dashed line), and the chorion (Figure 8B/h; blue arrowheads). Staining was also intense in blood vessels. However, in the CET 20 and LPS groups, staining intensity in these structures decreased significantly (Figure 8B/n–t; blue, yellow, and green arrowheads, red dashed line) (Table S1g). In the CET 20 and LPS groups, positive staining was observed in hematopoietic cells (Figure 8B/n–t; red arrowheads) and sinusoidal trophoblasts (Figure 8B/m–o; orange arrowheads).

3.15 | Western Blot Results of St2 Protein

3.15.1 | St2 protein Levels Were Decreased in the Cervix, Uterus, and Placenta in the Groups Treated With LPS and CET 20

The decrease in protein levels in the CET 20 and LPS groups was significant in all tissues ($p < 0.05$) (Figure 8C/a–c).

4 | Discussion

Preterm birth has been most frequently associated with infection in the literature. The most commonly proposed mechanism underlying infection-induced preterm labor is the increased colonization of vaginal pathogens [4], and LPS is frequently used in experimental animal models to mimic infection-mediated preterm labor. Observing lymphocyte infiltration and bleeding in tissues following LPS application are among the most frequently reported findings in the literature during preterm birth [6, 35]. Our previous study demonstrated that protein expression can vary, and different staining reactions can occur in the transition region between the cervix and uterus [6]. Our new study reveals that IL-33 expression is particularly intense in the cervix compared to the uterus during pregnancy. Again, in the nonpregnant group, the expression in the cervix is higher than in the pregnancy period, and in the LPS group, the expression decreases significantly. For the first time in the literature, we report the expression pattern of IL-33 in the cervix and its LPS-mediated depletion, suggesting a potential therapeutic target. Similarly, we observed that MC markers were impaired in the group administered high-dose CET, while these markers remained close to control levels after the use of low-dose CET. Our study highlights the dose-dependent effects of CET during pregnancy and their impact on MC function in LPS-mediated preterm birth. This work may help fill the missing gaps in understanding the mechanisms of preterm labor and provide insights for therapeutic interventions.

Placental membranes act as a physical barrier against LPS and microbial agents [36]. The mouse placenta typically consists of

four distinct layers: the decidua, junctional region, labyrinth region, and chorionic plate [37]. The labyrinth zone supports the differentiation of fetal erythrocytes, while the junctional region regulates erythropoietic differentiation [38, 39]. Trophoblast giant cells in the placenta are associated with uterine decidualization. Spongiotrophoblasts and trophoblastic glycogen cells are part of the endocrine structure and play a role in hormone regulation [40, 41]. MCs possess the unique ability to neutralize or degrade toxic proteins [42]. However, in our study, it was observed that MC function was impaired in the placenta during inflammation.

FcεRIα is involved in the degranulation of MCs [43]. Although there are no studies in the literature specifically examining the relationship between FcεRIα and preterm birth, Th2 regulation has been associated with MC degranulation and cytokine responses. The reduced presence of degranulated MCs, particularly in preterm birth groups, suggests that decreased expression of FcεRIα, one of the key proteins regulating degranulation, may impair MC activation and, consequently, the Th2 response. This impairment could trigger premature birth. Similar findings were observed in the LPS and CET 20 groups in the cervix and placenta. These results suggest that high doses of CET impair MC function, thereby amplifying the effects of LPS and further supporting its role in preterm birth. FcεRIγ activation in MCs mediates the initiation of three key signals: (1) degranulation of preformed granules containing chemical mediators such as histamine and β-hexosaminidase, (2) production of arachidonic acid metabolites such as PG, and (3) transcription of multiple cytokine genes, including IL-4 and IL-6. These reactions are closely linked to the anti-inflammatory response. FcεRIγ, a subunit shared by several antigen receptor families, is also associated with collagen receptors, highlighting its multifunctional role in immune signaling [44]. The increased expression of FcεRIγ observed in the cervix in the CET 20 and LPS groups, as well as in the uterus in the LPS group, may be aimed at promoting the chemotaxis of immune cells. This increase may also represent an effort by the physiological system to stimulate MC degranulation to balance the Th1/Th2 immune response. Conversely, the decrease in FcεRIγ expression observed in the placenta in these groups is thought to be associated with dysfunction in cells expressing FcεRIγ or an insufficient protective response due to inflammation.

The role of histamine in inflammatory processes remains to be fully elucidated [45]. Histamine is a pleiotropic mediator involved in numerous pathophysiological processes, including the regulation of inflammation [46]. MCs are multifunctional cells that serve as the body's primary histamine producers [47]. Studies in mice have shown that MC degranulation occurs during birth, with histamine concentrations in MCs peaking toward the end of pregnancy and returning to normal levels after birth [48]. When our findings were evaluated, HRH-1 protein levels were decreased at the tissue level in all groups, with a significant reduction observed in the uterus and placenta. At the tissue level, staining was intense in the epithelium, particularly in the MCs of the cervix uteri. The interaction between these structures may play a critical role in determining the severity of the inflammatory response. Furthermore, the significant reduction in HRH-1 protein levels observed in the CET 20 and LPS groups suggests that MCs were unable to initiate an adequate inflammatory response, likely due to insufficient histamine release. These findings also suggest that high doses of MC inhibitors, similar to the effects of LPS, may impair MC function.

IL-33, a specific ligand of St-2 [49], acts as a mucosal alarmin and is thought to play a critical role in both innate and adaptive immunity. It contributes to tissue homeostasis, responds to environmental stresses, and functions as a positive regulator in initiating and maintaining the Th2 immune response. In infection-induced inflammation, IL-33 is released from the uterine mucosa and triggers decidual B cells to produce anti-inflammatory molecules. During pregnancy, the IL-33/St-2 axis in B cells is reported as a critical mechanism for controlling inflammation-induced PTL [29]. Additionally, IL-33 is described as a proinflammatory yet T cell–stabilizing alarmin released during tissue remodeling [50]. In experimental models, IL-33-treated mice exhibited increased neutrophil migration into areas of inflammation and more effective bacterial clearance than untreated mice [51]. IL-33 is produced and secreted by damaged or necrotic endothelial and epithelial cells, stimulating immune cells that express its receptor, St-2 [52]. Moreover, a study reported that LPS inhibited T cell proliferation but emphasized that IL-33 could counteract this inhibitory effect by modulating apoptotic signaling pathways [53]. Conversely, downregulation of ST2 in chorioamnionitis membranes and amniotic fluid in cases of preterm labor due to infection may exacerbate the pro-inflammatory response in these patients [54].

A striking result of our study is that IL-33 was specifically expressed in the cervix, particularly in the epithelium. The literature generally indicates that IL-33 triggers an anti-inflammatory response to inflammation via St-2, and its deficiency negatively impacts neutrophil migration and tissue repair. Our findings suggest that the cervix and placenta are the tissues most affected by LPS application, with the observed decrease in tissue and protein levels associated with impaired anti-inflammatory responses. The reduction in IL-33 levels in the LPS group is thought to be related to worsening cellular and mucosal responses, including MCs. Literature suggests that the IL-33/St-2-mediated mechanism shifts the inflammatory response axis toward a Th1-dominant direction. Based on this, regional increases or decreases in IL-33 expression may reflect efforts to adapt to inflammation through improved adaptive responses or alternative mechanisms. The suppression of IL-33 expression, following the shift from a Th2 to a Th1-dominant response under increased inflammatory load, is also considered a possible outcome. Literature highlights the close relationship between IL-33/St-2 signaling and the Th2 response. Our study observed a significant decrease in St-2 protein levels in all tissues in both the CET20 and LPS groups. This decrease, believed to parallel the reduction in IL-33, was evaluated as a disruption of the St-2 axis in the epithelial and stromal regions, likely due to the receptor-ligand relationship. Compared to findings in the literature, the transmembrane form of St-2 is associated with managing the inflammatory process. Consequently, its deficiency may result in negative outcomes, particularly in the context of combating inflammation. In the literature, St-2 deficiency is linked to an increased Th1 response and efforts to modulate inflammation toward a Th2-dominant response. Based on this, the cervical and uterine responses observed in our study may reflect post-transition changes aimed at maintaining homeostasis by modulating St-2 expression to preserve the Th2 balance. While St-2 expression by MCs has been

previously reported, its expression in the cervix represents a novel contribution to the literature.

Secreted tryptases and chymases play crucial roles in regulating inflammation, matrix degradation, and tissue remodeling through various mechanisms. MCs maturing in different tissue microenvironments can exhibit significant variability in their express types and quantities of tryptases and chymases. McC and McT face the critical dilemma of preventing the spread of inflammation while avoiding triggering tissue damage. Such trade-offs are inherent to the actions of inflammatory mediators, including "Th2" cytokines [55, 56]. When evaluating the literature, chymase is noted to influence inflammatory cell function, although its role in protection against bacterial pathogens is less well understood. MCs secrete chymase as part of a defensive mechanism to reduce host susceptibility to systemic bacterial infections [57]. Additionally, constitutively released chymase may play a role in maintaining tissue homeostasis [58]. Tryptase levels in biological fluids are considered a marker of MC count and activation [59]. Although the exact mechanism of tryptase is not yet fully understood [60], the release of tryptase from activated MCs can amplify the inflammatory response by stimulating secretion from neighboring MCs [61].

Our McC findings demonstrate that expression levels at both the tissue and protein levels were reduced in the CET 20 and LPS groups, particularly in the cervix and uterus. In the placenta, the reduction was significant only in the LPS group. These results suggest that the role of MCs as either "friend" or "foe" during inflammation may depend on the severity of the inflammatory response. It is hypothesized that if McC expression, which plays a critical role in maintaining homeostasis during the inflammatory process, remains below the pathogen-limiting threshold, inflammation may be exacerbated. This supports the conclusion that MCs may be involved in regulating the Th2 response to mitigate tissue damage and resolve the inflammatory environment. The observed decrease in the CET 20 group indicates that high-dose CET administration suppresses MC function, supporting the tissue effects of LPS. The lower presence of MCs in the placenta compared to other tissues may explain the distinct response observed in this tissue. Additionally, less MC dysfunction in the placenta may promote a more positive inflammatory response. The control-like response observed in the CET 10 group is hypothesized to be related to this condition, suggesting that low-dose CET treatment preserves MC function and supports tissue homeostasis.

Additionally, McT expression was decreased in all tissues in the CET 20 and LPS groups. Tryptase expression was particularly attenuated in the LPS group, primarily in MCs colonizing the cervical orifice. This reduction may be linked to the intensity of Th1 activation, as well as MC dysfunction and suppression. Consequently, these cells, which are typically involved in modulating the immune response toward a Th2 direction, appear unable to restore the disrupted balance. According to the data, tryptase is directly related to the number and functionality of MCs. McT is essential for the release of histamine and other mediators necessary for controlling inflammation. In the LPS-treated groups, MC granules were retained or only partially released within the cytoplasm. This has been associated with a diminished capacity to control inflammation or initiate an anti-inflammatory response. This inability to fully release mediators may have contributed to the induction of preterm labor by failing to create the amplification required to stimulate neighboring MCs and by lacking sufficient mediators to limit inflammation. Furthermore, the failure of tryptase, which is critical in post-inflammatory tissue repair, to perform its function may negatively impact the resolution of inflammation and support tissue damage.

The most important finding from these data is that LPS-mediated preterm birth, which we associate with inflammation and pathogens, is closely linked to the doses of CET and the role of MCs in this process. The suppression of MC markers observed in both the high-dose CET and LPS groups suggests that changes in the number and activation of MCs impair their ability to limit the inflammatory reaction. This indicates that high-dose CET may support the inflammatory process and underscores the necessity of healthy MC function in controlling inflammation. The specific expression of IL-33 in the cervix, which was maintained in the low-dose CET group, was lost in the LPS group. This suggests that IL-33/St2 axis could be a promising target for reducing inflammation and preventing LPS-mediated preterm birth. Similarly, the association between MC markers and preterm birth highlights their potential predictive value for assessing inflammatory risk. Although further studies are needed to fully elucidate this complex process, our findings provide valuable new insights that can contribute to advancements in this field. These results may encourage the development of different experimental and clinical studies to explore the mechanisms underlying LPS-mediated preterm birth and the therapeutic potential of IL-33/St2 axis and MCs regulation.

Acknowledgments

We want to thank student Cemre Nur Balcı for her assistance. This research was supported by the Scientific and Technological Research Council of Turkey (TUBITAK, Project number 121S341, S.A.).

Ethics Statement

Approval was obtained from the Ethics Committee of Akdeniz University Animal Experiments Local Ethics Committee/24.05.2021-91. The procedures used in this study adhere to the tenets of the Declaration of Helsinki. We confirm the study is reported following ARRIVE guidelines.

Conflicts of Interest

The authors declare that the research was conducted without any commercial or financial relationships that could be construed as a potential conflict of interest.

Data Availability Statement

The data that support the findings of this study are available from the corresponding author upon reasonable request.

References

1. W. M. Callaghan, M. F. MacDorman, S. A. Rasmussen, C. Qin, and E. M. Lackritz, "The Contribution of Preterm Birth to Infant Mortality Rates in the United States," *Pediatrics* 118, no. 4 (2006): 1566–1573, https://doi.org/10.1542/peds.2006-0860.

2. WHO. Born Too Soon: The Global Action Report on Preterm Birth. 2023.

3. N. M. Nour, "Premature Delivery and the Millennium Development Goal," *Reviews in Obstetrics and Gynecology* 5, no. 2 (2012): 100–105.

4. R. L. Goldenberg, J. F. Culhane, J. D. Iams, and R. Romero, "Epidemiology and Causes of Preterm Birth," *Lancet* 371, no. 9606 (2008): 75–84, https://doi.org/10.1016/S0140-6736(08)60074-4.

5. R. Romero, S. K. Dey, and S. J. Fisher, "Preterm Labor: One Syndrome, Many Causes," *Science* 345, no. 6198 (2014): 760–765, https://doi.org/10.1126/science.1251816.

6. S. Avci, N. Kuscu, L. Kilinc, and I. Ustunel, "Relationship of Notch Signal, Surfactant Protein A, and Indomethacin in Cervix during Preterm Birth: Mast Cell and Jagged-2 May Be Key in Understanding Infection-mediated Preterm Birth," *Journal of Histochemistry and Cytochemistry* 70, no. 2 (2022): 121–138, https://doi.org/10.1369/00221554211061615.

7. D. R. Moritz, H. R. Rodewald, J. Gheyselinck, and R. Klemenz, "The IL-1 Receptor-related T1 Antigen Is Expressed on Immature and Mature Mast Cells and on Fetal Blood Mast Cell Progenitors," *Journal of Immunology* 161, no. 9 (1998): 4866–4874.

8. H. Cui, F. Liu, Y. Fang, T. Wang, B. Yuan, and C. Ma, "Neuronal FcepsilonRIalpha Directly Mediates Ocular Itch via IgE-Immune Complex in a Mouse Model of Allergic Conjunctivitis," *Journal of Neuroinflammation* 19, no. 1 (2022): 55, https://doi.org/10.1186/s12974-022-02417-x.

9. T. Rasmussen, J. F. Jensen, N. Ostergaard, D. Tanner, T. Ziegler, and P. O. Norrby, "On the Mechanism of the Copper-Catalyzed Cyclopropanation Reaction," *Chemistry (Weinheim An Der Bergstrasse, Germany)* 8, no. 1 (2002): 177–184, https://doi.org/10.1002/1521-3765(20020104)8:1⟨177::aid-chem177⟩3.0.co;2-h.

10. C. Kanellopoulos-Langevin, S. M. Caucheteux, P. Verbeke, and D. M. Ojcius, "Tolerance of the Fetus by the Maternal Immune System: Role of Inflammatory Mediators at the Feto-Maternal Interface," *Reproductive Biology and Endocrinology [Electronic Resource]: RB&E* 1 (2003): 121, https://doi.org/10.1186/1477-7827-1-121.

11. D. Sakurai, S. Yamasaki, K. Arase, et al., "Fc epsilon RI Gamma-ITAM Is Differentially Required for Mast Cell Function In Vivo," *Journal of Immunology* 172, no. 4 (2004): 2374–2381, https://doi.org/10.4049/jimmunol.172.4.2374.

12. E. Bytautiene, R. Romero, Y. P. Vedernikov, F. El-Zeky, G. R. Saade, and R. E. Garfield, "Induction of Premature Labor and Delivery by Allergic Reaction and Prevention by Histamine H1 Receptor Antagonist," *American Journal of Obstetrics and Gynecology* 191, no. 4 (2004): 1356–1361, https://doi.org/10.1016/j.ajog.2004.06.092.

13. J. G. Donahue, J. B. Lupton, and A. M. Golichowski, "Cutaneous Mastocytosis Complicating Pregnancy," *Obstetrics and Gynecology* 85, no. 5 Pt 2 (1995): 813–815, https://doi.org/10.1016/0029-7844(94)00305-w.

14. A. L. Sheffer and L. L. Samuels, "Cetirizine: Antiallergic Therapy Beyond Traditional H1 Antihistamines," *Journal of Allergy and Clinical Immunology* 86, no. 6 Pt 2 (1990): 1040–1046, https://doi.org/10.1016/s0091-6749(05)80251-9.

15. M. Meadows, "Pregnancy and the Drug Dilemma," *FDA Consumer* 35, no. 3 (2001): 16–20.

16. S. Kar, A. Krishnan, K. Preetha, and A. Mohankar, "A Review of Antihistamines Used During Pregnancy," *Journal of Pharmacology and Pharmacotherapeutics* 3, no. 2 (2012): 105–108, https://doi.org/10.4103/0976-500X.95503.

17. T. Shimizu, J. Nishihira, H. Watanabe, R. Abe, T. Ishibashi, and H. Shimizu, "Cetirizine, an H1-Receptor Antagonist, Suppresses the Expression of Macrophage Migration Inhibitory Factor: Its Potential Anti-Inflammatory Action," *Clinical and Experimental Allergy* 34, no. 1 (2004): 103–109, https://doi.org/10.1111/j.1365-2222.2004.01836.x.

18. F. E. Simons, "Recent Advances in H1-Receptor Antagonist Treatment," *Journal of Allergy and Clinical Immunology* 86, no. 6 Pt 2 (1990): 995–999, https://doi.org/10.1016/s0091-6749(05)80242-8.

19. F. Etwel, N. Djokanovic, M. E. Moretti, R. Boskovic, J. Martinovic, and G. Koren, "The Fetal Safety of Cetirizine: An Observational Cohort Study and Meta-Analysis," *Journal of Obstetrics and Gynaecology* 34, no. 5 (2014): 392–399, https://doi.org/10.3109/01443615.2014.896887.

20. C. Gilbert, P. Mazzotta, R. Loebstein, and G. Koren, "Fetal Safety of Drugs Used in the Treatment of Allergic Rhinitis: A Critical Review," *Drug Safety* 28, no. 8 (2005): 707–719, https://doi.org/10.2165/00002018-200528080-00005.

21. E. N. Charlesworth, A. Kagey-Sobotka, P. S. Norman, and L. M. Lichtenstein, "Effect of Cetirizine on Mast Cell-Mediator Release and Cellular Traffic During the Cutaneous Late-Phase Reaction," *Journal of Allergy and Clinical Immunology* 83, no. 5 (1989): 905–912, https://doi.org/10.1016/0091-6749(89)90104-8.

22. H. Wilkerson, P. Datta, K. Rewers-Felkins, T. Baker, and T. W. Hale, "Maternal Transfer of Cetirizine into Human Milk," *Journal of Human Lactation* 37, no. 1 (2021): 135–138, https://doi.org/10.1177/0890334420949847.

23. E. Khalilzadeh, F. Azarpey, and R. Hazrati, "The Effect of Histamine H1 Receptor Antagonists on the Morphine-Induced Antinociception in the Acute Trigeminal Model of Nociception in Rats," *Asian Journal of Pharmaceutical and Clinical Research* 10, no. 1 (2017): 1–5.

24. I. Rauter, M. T. Krauth, K. Westritschnig, et al., "Mast Cell-Derived Proteases Control Allergic Inflammation Through Cleavage of IgE," *Journal of Allergy and Clinical Immunology* 121, no. 1 (2008): 197–202, https://doi.org/10.1016/j.jaci.2007.08.015.

25. F. M. Menzies, C. A. Higgins, M. C. Shepherd, R. J. Nibbs, and S. M. Nelson, "Mast Cells Reside in Myometrium and Cervix, but Are Dispensable in Mice for Successful Pregnancy and Labor," *Immunology and Cell Biology* 90, no. 3 (2012): 321–329, https://doi.org/10.1038/icb.2011.40.

26. R. E. Garfield, A. M. Irani, L. B. Schwartz, E. Bytautiene, and R. Romero, "Structural and Functional Comparison of Mast Cells in the Pregnant versus Nonpregnant Human Uterus," *American Journal of Obstetrics and Gynecology* 194, no. 1 (2006): 261–267, https://doi.org/10.1016/j.ajog.2005.05.011.

27. M. Mobini, M. Mortazavi, S. Nadi, M. Zare-Bidaki, S. Pourtalebi, and M. K. Arababadi, "Significant Roles Played by Interleukin-10 in Outcome of Pregnancy," *Iranian Journal of Basic Medical Sciences* 19, no. 2 (2016): 119–124.

28. F. Y. Liew, J. P. Girard, and H. R. Turnquist, "Interleukin-33 in Health and Disease," *Nature Reviews Immunology* 16, no. 11 (2016): 676–689, https://doi.org/10.1038/nri.2016.95.

29. N. Valeff, L. Juriol, F. Quadrana, et al., "Expression of IL-33 Receptor Is Significantly Up-Regulated in B Cells during Pregnancy and in the Acute Phase of Preterm Birth in Mice," *Frontiers in Immunology* 11 (2020): 446, https://doi.org/10.3389/fimmu.2020.00446.

30. B. Griesenauer and S. Paczesny, "The ST2/IL-33 Axis in Immune Cells During Inflammatory Diseases," *Frontiers in Immunology* 8 (2017): 475, https://doi.org/10.3389/fimmu.2017.00475.

31. N. Valero-Pacheco, E. K. Tang, N. Massri, et al., "Maternal IL-33 Critically Regulates Tissue Remodeling and Type 2 Immune Responses in the Uterus During Early Pregnancy in Mice," *Proceedings of the National Academy of Sciences* 119, no. 35 (2022): e2123267119, https://doi.org/10.1073/pnas.2123267119.

32. M. Krystel-Whittemore, K. N. Dileepan, and J. G. Wood, "Mast Cell: A Multi-Functional Master Cell," *Frontiers in Immunology* 6 (2015): 620, https://doi.org/10.3389/fimmu.2015.00620.

33. F. E. Simons, "H1-receptor Antagonists: Clinical Pharmacology and Therapeutics," *Journal of Allergy and Clinical Immunology* 84, no. 6 Pt 1 (1989): 845–861, https://doi.org/10.1016/0091-6749(89)90377-1.

34. S. Avci, E. Golal, and N. Acar, "Evaluation of Changes of Apelin and Apelin Receptor (APJ) Expression in Cervix-Uterus and Placental Axis in an LPS-Induced Preterm Labor Model," *International Journal of Developmental Biology* 67, no. 3 (2023): 91–100, https://doi.org/10.1387/ijdb.230156sa.

35. L. F. Edey, K. P. O'Dea, B. R. Herbert, et al., "The Local and Systemic Immune Response to Intrauterine LPS in the Prepartum Mouse," *Biology of Reproduction* 95, no. 6 (2016): 125, https://doi.org/10.1095/biolreprod.116.143289.

36. H. S. Kim, J. H. Cho, H. W. Park, H. Yoon, M. S. Kim, and S. C. Kim, "Endotoxin-Neutralizing Antimicrobial Proteins of the Human Placenta," *Journal of Immunology* 168, no. 5 (2002): 2356–2364, https://doi.org/10.4049/jimmunol.168.5.2356.

37. S. M. Isaac, M. B. Langford, D. G. Simmons, and S. L. Adamson. *Anatomy of the Mouse Placenta throughout Gestation, in the Guide to Investigation of Mouse Pregnancy* (vol 4. Academic Press, 2014).

38. N. Azevedo Portilho and M. Pelajo-Machado, "Mechanism of Hematopoiesis and Vasculogenesis in Mouse Placenta," *Placenta* 69 (2018): 140–145, https://doi.org/10.1016/j.placenta.2018.04.007.

39. N. Azevedo Portilho, P. Tavares Guedes, B. A. Croy, and M. Pelajo-Machado, "Localization of Transient Immature Hematopoietic Cells to Two Distinct, Potential Niches in the Developing Mouse Placenta," *Placenta* 47 (2016): 1–11, https://doi.org/10.1016/j.placenta.2016.08.081.

40. D. Hu and J. C. Cross, "Development and Function of Trophoblast Giant Cells in the Rodent Placenta," *International Journal of Developmental Biology* 54, no. 2 (2010): 341–354, https://doi.org/10.1387/ijdb.082768dh.

41. M. Hemberger, C. W. Hanna, and W. Dean, "Mechanisms of Early Placental Development in Mouse and Humans," *Nature Reviews Genetics* 21, no. 1 (2020): 27–43, https://doi.org/10.1038/s41576-019-0169-4.

42. A. Dudeck, M. Koberle, O. Goldmann, et al., "Mast Cells as Protectors of Health," *Journal of Allergy and Clinical Immunology* 144, no. 4S (2019): S4–S18, https://doi.org/10.1016/j.jaci.2018.10.054.

43. E. A. Barbu, J. Zhang, E. H. Berenstein, J. R. Groves, L. M. Parks, and R. P. Siraganian, "The Transcription Factor Zeb2 Regulates Signaling in Mast Cells," *Journal of Immunology* 188, no. 12 (2012): 6278–6286, https://doi.org/10.4049/jimmunol.1102660.

44. H. Turner and J. P. Kinet, "Signalling Through the High-Affinity IgE Receptor Fc epsilonRI," *Nature* 402, no. Suppl 6760 (1999): B24–30, https://doi.org/10.1038/35037021.

45. N. Hirasawa, "Expression of Histidine Decarboxylase and Its Roles in Inflammation," *International Journal of Molecular Sciences* 20, no. 2 (2019): 376, https://doi.org/10.3390/ijms20020376.

46. B. Schirmer and D. Neumann, "The Function of the Histamine H4 Receptor in Inflammatory and Inflammation-Associated Diseases of the Gut," *International Journal of Molecular Sciences* 22, no. 11 (2021): 6116, https://doi.org/10.3390/ijms22116116.

47. E. B. Thangam, E. A. Jemima, H. Singh, et al., "The Role of Histamine and Histamine Receptors in Mast Cell-Mediated Allergy and Inflammation: The Hunt for New Therapeutic Targets," *Frontiers in Immunology* 9 (2018): 1873, https://doi.org/10.3389/fimmu.2018.01873.

48. L. Padilla, K. Reinicke, H. Montesino, et al., "Histamine Content and Mast Cells Distribution in Mouse Uterus: The Effect of Sexual Hormones, Gestation and Labor," *Cellular and Molecular Biology* 36, no. 1 (1990): 93–100.

49. L. Jeng, A. V. Yamshchikov, S. E. Judd, et al., "Alterations in Vitamin D Status and Anti-Microbial Peptide Levels in Patients in the Intensive Care Unit With Sepsis," *Journal of translational medicine* 7 (2009): 28, https://doi.org/10.1186/1479-5876-7-28.

50. I. A. Stelzer, M. S. Ghaemi, X. Han, et al., "Integrated Trajectories of the Maternal Metabolome, Proteome, and Immunome Predict Labor Onset," *Science Translational Medicine* 13, no. 592 (2021): eabd9898, https://doi.org/10.1126/scitranslmed.abd9898.

51. J. C. Alves-Filho, F. Sonego, F. O. Souto, et al., "Interleukin-33 Attenuates Sepsis by Enhancing Neutrophil Influx to the Site of Infection," *Nature Medicine* 16, no. 6 (2010): 708–712, https://doi.org/10.1038/nm.2156.

52. J. Schmitz, A. Owyang, E. Oldham, et al., "IL-33, an Interleukin-1-Like Cytokine That Signals via the IL-1 Receptor-Related Protein ST2 and Induces T Helper Type 2-Associated Cytokines," *Immunity* 23, no. 5 (2005): 479–490, https://doi.org/10.1016/j.immuni.2005.09.015.

53. C. Li, X. Yu, L. Zhang, et al., "The Potential Role and Regulatory Mechanism of IL-33/ST2 Axis on T Lymphocytes During Lipopolysaccharide Stimulation or Perinatal Listeria Infection," *International Immunopharmacology* 108 (2022): 108742, https://doi.org/10.1016/j.intimp.2022.108742.

54. T. Stampalija, T. Chaiworapongsa, R. Romero, et al., "Soluble ST2, a Modulator of the Inflammatory Response, in Preterm and Term Labor," *Journal of Maternal-Fetal & Neonatal Medicine* 27, no. 2 (2014): 111–121, https://doi.org/10.3109/14767058.2013.806894.

55. F. D. Finkelman, "The Other Side of the Coin: The Protective Role of the TH2 Cytokines," *Journal of Allergy and Clinical Immunology* 107, no. 5 (2001): 772–780, https://doi.org/10.1067/mai.2001.114989.

56. G. H. Caughey, "Mast Cell Tryptases and Chymases in Inflammation and Host Defense," *Immunological Reviews* 217 (2007): 141–154, https://doi.org/10.1111/j.1600-065X.2007.00509.x.

57. C. Gendrin, N. J. Shubin, E. Boldenow, et al., "Mast Cell Chymase Decreases the Severity of Group B Streptococcus Infections," *Journal of Allergy and Clinical Immunology* 142, no. 1 (2018): 120–129.e6, https://doi.org/10.1016/j.jaci.2017.07.042.

58. E. Tchougounova, G. Pejler, and M. Abrink, "The Chymase, Mouse Mast Cell Protease 4, Constitutes the Major Chymotrypsin-Like Activity in Peritoneum and Ear Tissue. A Role for Mouse Mast Cell Protease 4 in Thrombin Regulation and Fibronectin Turnover," *Journal of Experimental Medicine* 198, no. 3 (2003): 423–431, https://doi.org/10.1084/jem.20030671.

59. L. B. Schwartz, "Clinical Utility of Tryptase Levels in Systemic Mastocytosis and Associated Hematologic Disorders," *Leukemia Research* 25, no. 7 (2001): 553–562, https://doi.org/10.1016/s0145-2126(01)00020-0.

60. I. Fajardo and G. Pejler, "Formation of Active Monomers From Tetrameric human Beta-tryptase," *Biochemical Journal* 369, no. Pt 3 (2003): 603–610, https://doi.org/10.1042/BJ20021418.

61. S. He, M. D. Gaca, and A. F. Walls, "A Role for Tryptase in the Activation of human Mast Cells: Modulation of Histamine Release by Tryptase and Inhibitors of Tryptase," *Journal of Pharmacology and Experimental Therapeutics* 286, no. 1 (1998): 289–297.

Supporting Information

Additional supporting information can be found online in the Supporting Information section.